Nodeless High-T_c Superconductivity in the Highly Overdoped CuO_2 Monolayer

Kun Jiang,[1,2] Xianxin Wu,[2,3,*] Jiangping Hu,[2,4,5,†] and Ziqiang Wang[1,‡]
[1]Department of Physics, Boston College, Chestnut Hill, Massachusetts 02467, USA
[2]Beijing National Laboratory for Condensed Matter Physics and Institute of Physics, Chinese Academy of Sciences, Beijing 100190, China
[3]Institut für Theoretische Physik und Astrophysik, Julius-Maximilians-Universität Würzburg, 97074 Würzburg, Germany
[4]Collaborative Innovation Center of Quantum Matter, Beijing 100871, China
[5]Kavli Institute of Theoretical Sciences, University of Chinese Academy of Sciences, Beijing 100190, China

(Received 18 June 2018; published 29 November 2018)

We study the electronic structure and superconductivity in a CuO_2 monolayer grown recently on the d-wave cuprate superconductor $Bi_2Sr_2CaCu_2O_{8+\delta}$. Density functional theory calculations indicate a significant charge transfer across the interface such that the CuO_2 monolayer is heavily overdoped into the hole-rich regime yet inaccessible in bulk cuprates. We show that both the Cu $d_{x^2-y^2}$ and $d_{3z^2-r^2}$ orbitals become important and the Fermi surface contains one electron and one hole pocket associated with the two orbitals, respectively. Constructing a minimal correlated two-orbital model for the e_g complex, we show that the spin-orbital exchange interactions produce a nodeless superconductor with extended s-wave pairing symmetry and a pairing energy gap comparable to the bulk d-wave gap, in agreement with recent experiments. The findings point to a direction of realizing new high-T_c superconductors in ozone grown transition-metal-oxide monolayer heterostructures.

DOI: 10.1103/PhysRevLett.121.227002

The commonly held belief of the high-T_c cuprate superconducting (SC) state [1] is that the superconductivity originates from two-dimensional copper-oxide (CuO_2) planes with a nodal d-wave pairing symmetry [2–4]. In a recent attempt to directly probe the SC state in the copper-oxide plane, a CuO_2 monolayer on $Bi_2Sr_2CaCu_2O_{8+\delta}$ (Bi2212) has been grown successfully by state-of-the-art ozone molecular beam epitaxy (MBE) [5]. In contrast to the widely observed V-shaped local density of states (LDOS) typical of a nodal d-wave pairing gap in bulk cuprates, scanning tunneling microscopy (STM) on the CuO_2 monolayer reveals a robust U-shaped LDOS characteristic of a nodeless SC gap, which is further shown to be insensitive to nonmagnetic impurities [5]. Several theoretical scenarios have been proposed for this remarkable observation, largely based on the SC proximity effect but with the d-wave nodes avoided by different Fermi surfaces or coexisting magnetism in the monolayer [6–9]. Here, we propose a different scenario. We argue that the CuO_2 monolayer has a new electronic structure due to interface charge transfer and exhibits an intrinsic nodeless, s-wave SC state. Thus, while the monolayer may not be representative of the bulk CuO_2 layers, it has potentially realized the direction of finding new and novel forms of high-T_c superconductors in transition-metal-oxide heterostructures by interface charge transfer.

The main findings are summarized in the schematic phase diagram shown in Fig. 1. The left side of Fig. 1 has been realized by hole doping the antiferromagnetic (AFM) parent state in bulk cuprates, where the $3d^9$ Cu^{2+} has three e_g electrons ($n_e = 3$) occupying the well-split $d_{x^2-y^2}$ (d_{x^2}) and $d_{3z^2-r^2}$ (d_{z^2}) orbitals due to Jahn-Teller distortion. The d-wave superconductor emerges under the SC dome with a maximum T_c around an optimal doping concentration $x_h \sim 0.16$. Experiments show that the metallic state in bulk cuprates has a single band of the d_{x^2} character [10] crossing the Fermi level. Note that heavy overdoping is difficult and the region with $x_h > 0.3$ has not been accessible in bulk cuprates.

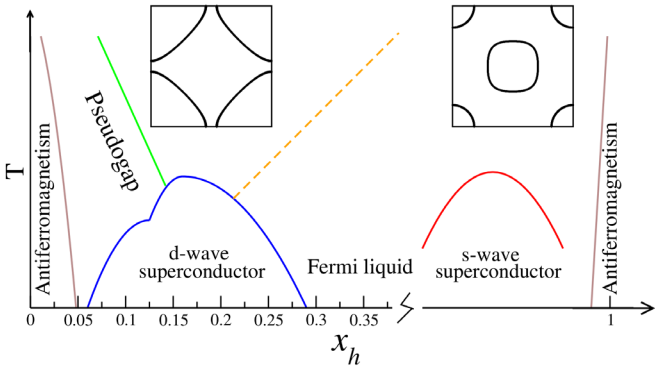

FIG. 1. Schematic phase diagram as a function of hole doping x_h, contrasting the single-band d-wave SC phase realized in bulk cuprates (left side) with the two-orbital nodeless SC phase in the hole-rich monolayer CuO_2/Bi2212 (right side). The corresponding FS is shown in the insets.

The right side of Fig. 1 is conjectured for the monolayer CuO_2/Bi2212. Based on the experimental evidence suggesting that the monolayer crystalizes into CuO_2 [5], a significant charge transfer must occur between the CuO_2 monolayer and the Bi2212 substrate in order to maintain charge neutrality. We will show that this is indeed supported by density functional theory (DFT) calculations and charge-transfer correlations. Thus, the CuO_2 monolayer is highly overdoped and reaches a regime yet inaccessible in bulk cuprates. As shown in Fig. 1, this hole-rich regime approaches $3d^8$ (Cu^{3+}) with $n_e = 2$ in the two e_g orbitals. We show that both d_{x^2} and d_{z^2} orbitals become active and the electronic structure requires a minimal two-band description with one electron FS enclosing Γ and one hole FS around M (Fig. 1). Constructing a two-orbital Hubbard model and studying its SC properties using both the weak- and strong-coupling approaches, we find that the hole-rich CuO_2 monolayer is a multiband nodeless superconductor driven by both spin-spin and spin-orbital-entangled (super)exchange interactions. The pairing energy gaps are comparable in magnitude to the bulk d-wave gap and exhibit a sign change on the two FSs, analogous to Fe-based superconductors. The calculated STM conductance displays the U-shaped spectrum consistent with the experimental observations.

We first carry out a DFT calculation to simulate a CuO_2 monolayer on Bi2212 using the Vienna *ab initio* simulation package (VASP) [11–15]. The details are given in Supplemental Material [16]. As illustrated in Fig. 2(a), due to the missing apical oxygen in the unbalanced octahedron, the cation Cu attracts the bottom anion oxygen (O_a) and shortens the out-of-plane Cu—O_a distance at the interface to 2.11 Å, after relaxation. This value is close to the in-plane Cu—O bond length of 1.92 Å, which is much shorter than the 2.82 Å Cu—O_a distance in the bulk. The point group symmetry D_{4h} also breaks down to C_{4v}. There are two immediate consequences. (i) The p_z orbital of the bottom O_a strongly hybridizes with the Cu d_{z^2} orbital. This leads to a d_{z^2} -like bonding orbital and transfers charges to the oxygen in the BiO layer. The excess charge transfer causes the Cu valence in the monolayer to approach $3d^8$ (Cu^{3+}) with two electrons occupying the e_g orbitals. (ii) The crystal field splitting between the d_{x^2} and d_{z^2} orbitals is significantly reduced compared to in the bulk.

These phenomena show up in the calculated band structure shown in Fig. 2(b). The band highlighted by red markers contains the d_{x^2} orbital mixed with the antisymmetric combination of the in-plane oxygen p_x and p_y orbitals [10]. We label this band as the d_{x^2} band, which is heavily overdoped and electronlike near the zone center Γ. The green markers indicate the d_{z^2} band of the Cu d_{z^2} orbital mixed with the anion oxygen p_z orbital. It is holelike near the zone corner M, with its band top very close to the Fermi level. Thus, the monolayer CuO_2/Bi2212 has a different electronic structure than

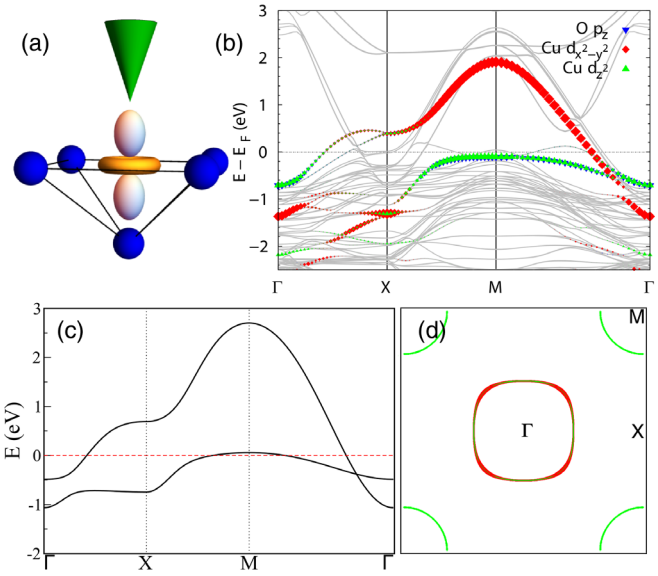

FIG. 2. (a) Atomic structure of the CuO_2 monolayer. The copper d_{z^2} orbital is shown in gold and silver (d_{x^2} not shown). Blue balls are oxygen ions. The oxygen (O_a) at the bottom of pyramid is in the BiO_2 layer of the Bi2212 substrate. (b) Band structure of the monolayer CuO_2/Bi2212 obtained using DFT. The orbital content of dispersions is color coded with red (d_{x^2}), green (d_{z^2}), and blue (p_z strongly hybridized with d_{z^2}). (c) Band dispersion of the two-orbital TB model with the FS shown in (d) at $x_h = 0.9$ in the same color scheme.

the CuO_2 layer in the bulk. Note that, in the experiments [5], the CuO_2 monolayer is MBE grown on Bi2212 substrates that are optimally hole doped by the excess oxygen dopants, of which a substantial fraction resides near the BiO layers [17,18]. Their density is further increased in the top BiO layer in the ozone environment. As a result, an additional charge transfer takes place via the oxygen dopants hole doping the CuO_2 monolayer across the interface, which further stabilizes the CuO_2 structure and pushes the chemical potential into the d_{z^2} band. Consequently, the doped holes physically occupy both d_{x^2} and d_{z^2} orbitals, giving rise to one electron FS pocket around Γ and one hole pocket around M at the Fermi energy. In the cuprate terminology, the CuO_2 monolayer corresponds to the heavily overdoped, hole-rich region yet unreachable in bulk materials where the d_{z^2} orbital and d-d excitations play only a limited role [19–28].

We next construct a minimal two-orbital Hamiltonian $H = H_t + H_I$ for the CuO_2 monolayer, where H_t is a tight-binding (TB) model for the band structure and H_I describes the electronic correlations. Using $d_{\alpha\sigma}$, $\alpha = x, z$ to denote a spin-σ electron in the d_{x^2} and d_{z^2} orbitals,

$$H_t = \sum_{k\alpha\beta\sigma} \varepsilon_k^{\alpha\beta} d_{k\alpha\sigma}^{\dagger} d_{k\beta\sigma} + e_z \sum_{k\sigma} d_{kz\sigma}^{\dagger} d_{kz\sigma}, \qquad (1)$$

where e_z is the crystal field splitting between the two orbitals. We consider up to third nearest neighbor hopping

such that the kinetic energy of intraorbital hopping in Eq. (1) is $\varepsilon_k^{\alpha\alpha} = -2t_\alpha\gamma_k - 4t'_\alpha\alpha_k - 2t''_\alpha\gamma'_k$ with lattice harmonics of A_1 symmetry $\gamma_k = \cos k_x + \cos k_y$, $\alpha_k = \cos k_x \cos k_y$, and $\gamma'_k = \cos 2k_x + \cos 2k_y$. Because of the different orbital symmetry, the interorbital hopping leads to $\varepsilon_k^{xz} = 2t_{xz}\beta_k + 2t''_{xz}\beta'_k$, with B_1 harmonics $\beta_k = \cos k_x - \cos k_y$ and $\beta'_k = \cos 2k_x - \cos 2k_y$. The parameters of the TB model are given in Supplemental Material [16], and the chemical potential is treated as an independent variable. The TB band structure is shown in Fig. 2(c) at doping $x_h = 0.9$ or $n_e = 2.1$. It describes the DFT results in Fig. 2(b) very well. The FS is plotted in Fig. 2(d), showing one electron pocket around Γ and one hole pocket around M. Since ε_k^{xz} has d-wave form factors, the FS around Γ is mostly d_{x^2} -like around nodal but of a mixed character around antinodal directions. The hole pocket around M is mainly d_{z^2} -like, since the bands are well separated in energy there. The smaller overlap of out-of-plane orbitals makes the d_{z^2} band narrow with a small bandwidth, consistent with the DFT dispersions.

The correlation part follows from the standard two-orbital Hubbard model [29,30] for the e_g complex:

$$H_I = U\sum_{i,\alpha}\hat{n}_{i\alpha\uparrow}\hat{n}_{i\alpha\downarrow} + \left(U' - \frac{1}{2}J_H\right)\sum_{i,\alpha<\beta}\hat{n}_{i\alpha}\hat{n}_{i\beta} - J_H\sum_{i,\alpha\neq\beta}\mathbf{S}_{i\alpha}\cdot\mathbf{S}_{i\beta} + J_H\sum_{i,\alpha\neq\beta}d^\dagger_{i\alpha\uparrow}d^\dagger_{i\alpha\downarrow}d_{i\beta\downarrow}d_{i\beta\uparrow}, \quad (2)$$

where the intra- and interorbital Coulomb U and U', respectively, are related to Hund's coupling J_H by $U = U' + 2J_H$.

The emergence of the low-energy d_{z^2} band and the hole FS pocket around M enables an analogy to multiorbital nodeless Fe-pnictide superconductors [31–39], particularly when the correlation effects in Eq. (2) are treated using weak-coupling approaches. Since perfect nesting between the electron and hole pockets is absent, the only logarithmic divergence is in the Cooper channel. Following Ref. [34], we performed a two-patch renormalization group analysis and found that the nodeless s-wave superconductivity is the leading instability. Moreover, the relevant pair scattering across the electron and hole FS, i.e., the u_3 channel [34], drives a sign-changing $s_\pm$ gap function on the two FS pockets.

An important difference between the Fe-based and cuprate superconductors is, however, that the former are p-d charge-transfer metals, whereas the latter are charge-transfer insulators [39]. Indeed, the nodeless SC state of the monolayer CuO_2/Bi2212 emerges [5] inside a charge-transfer gap of similar magnitude as in bulk cuprates [40]. It is thus necessary to carry out a strong-coupling study of the two-orbital Hubbard model. To this end, we derive in Supplemental Material the general spin-orbital superexchange interactions of the Kugel-Khomskii type [16,29,41]:

$$H_{J-K} = \sum_{\langle ij\rangle}\left(J\mathbf{S}_i\cdot\mathbf{S}_j + \sum_{\mu\nu}I_{\mu\nu}T_i^\mu T_j^\nu + \sum_{\mu\nu}K_{\mu\nu}(\mathbf{S}_i\cdot\mathbf{S}_j)(T_i^\mu T_j^\nu)\right), \quad (3)$$

where $\mathbf{S}_i$ is the spin-1/2 operator and T_i^μ, $\mu = 0, x, y, z$, are the orbital pseudospin-1/2 operators in the orbital basis $(|x^2-y^2\rangle, |z^2\rangle)^T$ [41]. In Eq. (3), the J term is the SU(2) invariant Heisenberg spin exchange coupling, while the terms proportional $I_{\mu\nu}$ and $K_{\mu\nu}$ describe the anisotropic orbital and spin-orbital-entangled superexchange interactions, respectively, since the orbital or pseudospin rotation symmetry is broken by the generic hoppings and crystal field in H_t. We thus arrive at an effective two-orbital strong-coupling model

$$H = P_G H_t P_G + H_{J-K}, \quad (4)$$

where P_G stands for the Gutzwiller projection of states with multiple occupations. Hereafter, we consider Eq. (4) as an effective low-energy theory for the hole-rich regime of the CuO_2 monolayer and study the emergent SC state due to the spin-orbit superexchange correlations. The Gutzwiller projection is treated in Supplemental Material [16] using the variational Gutzwiller approximation [42–44] for a generic set of interactions $U = 2.5$ eV and $J_H = 0.1U$.

The intersite quantum spin-orbital fluctuations described by Eq. (3) can be projected into the spin-singlet channel by $P_{ij}^s = \mathbf{S}_i\cdot\mathbf{S}_j - 1/4$ and written in terms of the pairing operators $\Delta_{ij}^{\alpha\beta\dagger} = d^\dagger_{i\alpha\uparrow}d^\dagger_{j\beta\downarrow} - d^\dagger_{i\alpha\downarrow}d^\dagger_{j\beta\uparrow}$. Since the d_{x^2} and d_{z^2} orbitals are split by the crystal field, there is an orbital order that causes the operator T_{iz} in Eq. (3) to take on its expectation value $1/2$. As shown in Supplemental Material [16], this leads to a spin exchange interaction corresponding to that of the Heisenberg term in the t-J model [2] with the familiar result $J_s(\mathbf{S}_i\cdot\mathbf{S}_j - \frac{1}{4}n_in_j) = -(J_s/2)\sum_{\alpha\beta}\Delta_{ij}^{\alpha\beta\dagger}\Delta_{ij}^{\alpha\beta}$. We set $J_s = 120$ meV, the commonly accepted value for bulk cuprates [2]. However, the T_{iz} order does not quench the transverse orbital fluctuations represented by $T_i^\pm$ that contribute to pairing. Remarkably, such spin-orbit-entangled, quadruple exchange interactions in Eq. (3) generate a new pairing contribution

$$KP_{ij}^s(T_i^+T_j^+ + \text{H.c.}) = -\frac{K}{2}(\Delta_{ij}^{xx\dagger}\Delta_{ij}^{zz} + \text{H.c.}), \quad (5)$$

which captures the physics of the interorbital pair scattering. This is the strong-coupling counterpart of the inter-FS pocket pair scattering in weak-coupling approaches [20,34]. We considered all spin-singlet pairing in Supplemental Material [16] and determined the expectation values of the pairing fields $\langle\Delta_{ij}^{\alpha\beta}\rangle$ self-consistently in the Gutzwiller approximation. The latter has the form

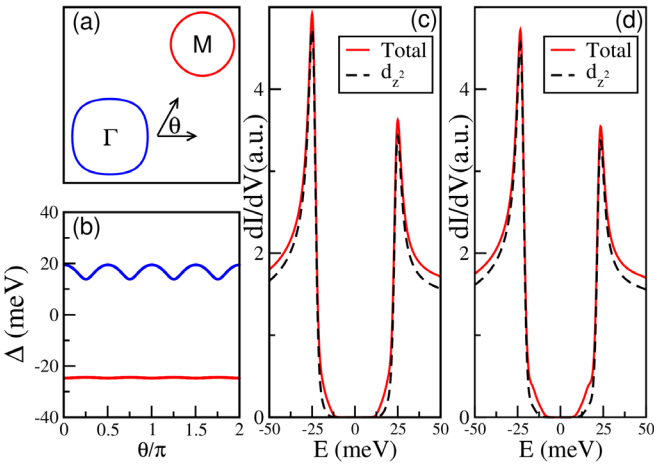

FIG. 3. (a) Normal state FS at $x_h = 0.9$. (b) SC pairing energy gaps at $K = 80$ meV along FS pockets with angle θ defined in (a). (c) U-shaped total LDOS (red solid line) showing a nodeless gap of about 25 meV. The LDOS from the d_{z^2} orbital is shown as dashed lines. (d) The same as in (c) obtained for $K = 60$ meV.

$$\langle \Delta_{ij}^{\alpha\beta} \rangle = \frac{1}{N_s} \sum_{\mathbf{k},\alpha\beta} \Delta_{\alpha\beta} b_{\alpha\beta}(\mathbf{k}) e^{i\mathbf{k}(r_i - r_j)}, \tag{6}$$

where N_s is the number of lattice sites and $b_{\alpha\beta}(k)$ the form factors of different symmetries in the C_{4v} point group of the crystal. For nearest neighbor pairing, $b_{\alpha\alpha}(k) = \gamma_k$ and $b_{xz}(k) = \beta_k$ in the A_1 symmetry channel, whereas $b_{\alpha\alpha}(k) = \beta_k$ and $b_{xz}(k) = \gamma_k$ in the B_1 channel. Our results show that the variational ground state in the strong-coupling theory is a nodeless superconductor with A_1 symmetry in the hole-rich regime where the FS contains both electron and hole pockets. Moreover, the pairing fields are dominated by the intraorbital $\Delta_{\alpha\alpha}$ with extended s-wave form factor $b_{\alpha\alpha} = \gamma_k$ in Eq. (6). In Figs. 3(a) and 3(b), we show the FS at $x_h = 0.9$ and the pairing energy gaps as a function of the angle along the two FS pockets for $K = 80$ meV. The nodeless $s_\pm$ gap function with opposite signs and comparable magnitude is a remarkable consequence of the spin-orbital-entangled exchange pairing interaction K in Eq. (5). The momentum space anisotropy of the gap function is small and more apparent on the electron pocket around Γ, which is larger and less circular. Such a nodeless multiorbital superconductor in the hole-rich regime is proposed in Fig. 1 for the monolayer CuO_2/Bi2212.

To compare to STM, we calculate the LDOS for each orbital $N_\alpha(\omega) = \sum_{k\sigma} \mathrm{Im} \int_0^\beta e^{i\omega\tau} \langle T_\tau d_{k\alpha\sigma}(\tau) d_{k\alpha\sigma}^\dagger(0) \rangle$. The total LDOS, $N(\omega) = N_x(\omega) + N_z(\omega)$, is shown in Fig. 3(c). It has a U-shaped spectrum with a pair of coherence peaks demarcating a nodeless energy gap around 25 meV, in good agreement with STM observations [5]. The LDOS from the d_{z^2} orbital, also shown in Fig. 3(c), has a slightly larger onset spectral gap and the majority of the total differential conductance due to the large DOS of the d_{z^2} band. Figure 3(d) shows the LDOS spectra obtained for a smaller $K = 60$ meV. The smaller onset spectral gap associated with the d_{x^2} orbital is visible, but the tunneling conductance, especially that into the d_{z^2} orbital, continues to exhibit the U-shaped spectrum. The tunneling matrix element on top of the monolayer also favors a path through the out-of-plane Cu $3d_{z^2}$ orbital as depicted in Fig. 2(a). The overall agreement with the STM findings supports our conjecture that the electronic structure and correlation in the monolayer CuO_2/Bi2212 produce an intrinsic two-orbital nodeless s-wave SC state.

The proposed two-orbital nodeless SC state near Cu $3d^8$ is different from the single-orbital extended s-wave pairing state known to arise with a very small pairing amplitude in the overdoped single-band t-J model [2,45]. To verify this point, we studied the intermediate doping regime $0.3 < x_h < 0.7$, where the d_{z^2} hole pocket has disappeared following a Lifshitz transition and the FS contains a single d_{x^2} electron pocket enclosing Γ [Fig. S1(c) in Supplemental Material]. The SC state indeed has extended s-wave pairing amplitudes that are 2 orders of magnitude smaller due to the suppression of orbital fluctuations. The electron pocket grows with reducing doping and transitions to a large hole FS around M for $x_h < 0.3$, where the nodal d-wave SC state is recovered as in the bulk cuprates. Finally, when the two-orbital model is studied at $x_h = 1$, i.e., in the Cu $3d^8$ limit with two electrons in the e_g complex, the Gutzwiller projected Hamiltonian $P_G H_t P_G$ has an insulating ground state with AFM long-range order for our parameters as indicated in the phase diagram in Fig. 1. This is consistent with the high-spin Mott insulating state of the two-orbital Hubbard model at half filling [46–49], where the AFM spin moments from the two orbitals are ferromagnetically aligned by J_H [50].

In conclusion, we proposed that the ozone MBE grown CuO_2 monolayer on Bi2212 is heavily overdoped due to interface charge transfer, reaching the hole-rich regime yet inaccessible in bulk cuprates. The resulting electronic structure involves holes occupying both Cu $3d_{x^2}$ and $3d_{z^2}$ orbitals. The quantum fluctuations of the spin-orbital superexchange interaction are shown to produce a two-orbital nodeless superconductor with a U-shaped LDOS and a comparably sized pairing gap as in bulk Bi2212 near optimal doping, providing a natural explanation of the STM experiments [5]. Although the SC proximity effect between a d-wave cuprate and a normal metal is difficult to achieve in c-axis-oriented junctions [51] and more detailed studies are necessary, it is reasonable to expect the intrinsic nodeless SC state of the CuO_2 monolayer to establish phase coherence with the bulk d-wave superconductor through inhomogeneous Josephson coupling at the interface. A possible mechanism to facilitate the interface charge transfer is through the type-B oxygen dopants in Bi2212 [17], residing close to the BiO layer as observed by STM [18]. Ozone MBE growth can increase significantly the type-B

dopants on the surface BiO layer, which in turn provide heavy hole doping for the capping CuO_2 monolayer. The predictions can be tested experimentally by measuring the quasiparticle band dispersion using angle-resolved photoemission spectroscopy or STM quasiparticle interference on samples with large enough coverage of a high-quality CuO_2 monolayer. Indeed, interface charge transfer and the change of FS topology have been observed recently with enhanced T_c in FeSe monolayer superconductors grown on a $SrTiO_3$ substrate [52–55]. It would also be interesting to probe and study the phonon dynamics and electron-phonon coupling at the interface [56]. The findings presented here provide insights for a new direction of searching for high-T_c superconductors in extended doping regimes and with liberated orbital degrees of freedom in ozone MBE grown transition-metal-oxide heterostructures.

We thank Sen Zhou and Andy Millis for helpful discussions. This work is supported in part by the Ministry of Science and Technology of China 973 program (No. 2017YFA0303100 and No. 2015CB921300), National Science Foundation of China (Grants No. NSFC-1190020, No. 11534014, and No. 11334012), the Strategic Priority Research Program of CAS (Grant No. XDB07000000), and the U.S. Department of Energy, Basic Energy Sciences Grant No. DE-FG02-99ER45747 (K. J. and Z. W.). Z. W. thanks the hospitality of Institute of Physics (IOP), Chinese Academy of Sciences (CAS), and Aspen Center for Physics and the support of NSF Grant No. PHY-1066293.

*xianxin.wu@physik.uni-wuerzburg.de
†jphu@iphy.ac.cn
‡wangzi@bc.edu

[1] J. G. Bednorz and K. A. Muller, Z. Phys. B **64**, 189 (1986).
[2] P. A. Lee, N. Nagaosa, and X.-G. Wen, Rev. Mod. Phys. **78**, 17 (2006).
[3] C. C. Tsuei, J. R. Kirtley, C. C. Chi, L. S. Yu-Jahnes, A. Gupta, T. Shaw, J. Z. Sun, and M. B. Ketchen, Phys. Rev. Lett. **73**, 593 (1994).
[4] C. C. Tsuei and J. R. Kirtley, Rev. Mod. Phys. **72**, 969 (2000).
[5] Y. Zhong, Y. Wang, S. Han, Y. Lv, W. Wang, D. Zhang, H. Ding, Y. Zhang, L. Wang, K. He, R. Zhong, J. A. Schneeloch, G. Gu, C. Song, X. Ma, and Q. K. Xue, Sci. Bull. **61**, 1239 (2016).
[6] G.-Y. Zhu, F.-C. Zhang, and G.-M. Zhang, Phys. Rev. B **94**, 174501 (2016).
[7] G. Zhu, Z. Wang, and G. Zhang, Europhys. Lett. **118**, 37004 (2017).
[8] Y. Wang, Z.-H. Wang, and W.-Q. Chen, Phys. Rev. B **96**, 104507 (2017).
[9] S. Wang, L. Zhang, and F. Wang, Phys. Rev. B **97**, 035112 (2018).
[10] F. C. Zhang and T. M. Rice, Phys. Rev. B **37**, 3759(R) (1988).
[11] G. Kresse and J. Hafner, Phys. Rev. B **47**, 558 (1993).
[12] G. Kresse and J. Furthmuller, Comput. Mater. Sci. **6**, 15 (1996).
[13] G. Kresse and J. Furthmuller, Phys. Rev. B **54**, 11169 (1996).
[14] J. P. Perdew, K. Burke, and M. Ernzerhof, Phys. Rev. Lett. **77**, 3865 (1996).
[15] H. J. Monkhorst and J. Pack, Phys. Rev. B **13**, 5188 (1976).
[16] See Supplemental Material at http://link.aps.org/supplemental/10.1103/PhysRevLett.121.227002 for more detailed discussions.
[17] S. Zhou, H. Ding, and Z. Wang, Phys. Rev. Lett. **98**, 076401 (2007).
[18] I. Zeljkovic, Z. Xu, J. S. Wen, G. D. Gu, R. S. Markiewicz, and J. E. Hoffman, Science **337**, 320 (2012).
[19] W. Weber, Z. Phys. B **70**, 323 (1988).
[20] D. L. Cox, M. Jarrell, C. Jayaprakash, H. R. Krishna-murthy, and J. Deisz, Phys. Rev. Lett. **62**, 2188 (1989).
[21] F. Buda, D. L. Cox, and M. Jarrell, Phys. Rev. B **49**, 1255 (1994).
[22] L. F. Feiner, M. Grilli, and C. Di Castro, Phys. Rev. B **45**, 10647 (1992).
[23] J. Zaanen and A. M. Oles, Phys. Rev. B **48**, 7197 (1993).
[24] R. Raimondi, J. H. Jefferson, and L. F. Feiner, Phys. Rev. B **53**, 8774 (1996).
[25] C.-C. Chen *et al.*, Phys. Rev. Lett. **105**, 177401 (2010).
[26] X. Wang, H. T. Dang, and A. J. Millis, Phys. Rev. B **84**, 014530 (2011).
[27] H. Sakakibara, H. Usui, K. Kuroki, R. Arita, and H. Aoki, Phys. Rev. Lett. **105**, 057003 (2010).
[28] H. Sakakibara, H. Usui, K. Kuroki, R. Arita, and H. Aoki, Phys. Rev. B **85**, 064501 (2012).
[29] C. Castellani, C. R. Natoli, and J. Ranninger, Phys. Rev. B **18**, 4945 (1978).
[30] A. Georges, L. de Medici, and J. Mravlje, Annu. Rev. Condens. Matter Phys. **4**, 137 (2013).
[31] I. I. Mazin, D. J. Singh, M. D. Johannes, and M. H. Du, Phys. Rev. Lett. **101**, 057003 (2008).
[32] S. Graser, T. A. Maier, P. J. Hirschfeld, and D. J. Scalapino, New J. Phys. **11**, 025016 (2009).
[33] F. Wang, H. Zhai, Y. Ran, A. Vishwanath, and D.-H. Lee, Phys. Rev. Lett. **102**, 047005 (2009).
[34] A. V. Chubukov, D. V. Efremov, and I. Eremin, Phys. Rev. B **78**, 134512 (2008).
[35] K. Seo, B. A. Bernevig, and J. Hu, Phys. Rev. Lett. **101**, 206404 (2008).
[36] W.-Q. Chen, K.-Y. Yang, Y. Zhou, and F.-C. Zhang, Phys. Rev. Lett. **102**, 047006 (2009).
[37] H. Kontani and S. Onari, Phys. Rev. Lett. **104**, 157001 (2010).
[38] Y. Yanagi, Y. Yamakawa, and Y. Ono, Phys. Rev. B **81**, 054518 (2010).
[39] S. Zhou, G. Kotliar, and Z. Wang, Phys. Rev. B **84**, 140505 (R) (2011).
[40] P. Cai, W. Ruan, Y. Peng, C. Ye, X. Li, Z. Hao, X. Zhou, D. Lee, and Y. Wang, Nat. Phys. **12**, 1047 (2016).
[41] K. I. Kugel and D. I. Khomskii, Sov. Phys. Usp. **25**, 231 (1982) [Sov. Phys. JETP **37**, 725 (1973)].
[42] J. Bunemann, W. Weber, and F. Gebhard, Phys. Rev. B **57**, 6896 (1998).

[43] F. Lechermann, A. Georges, G. Kotliar, and O. Parcollet, Phys. Rev. B **76**, 155102 (2007).
[44] S. Zhou and Z. Wang, Phys. Rev. Lett. **105**, 096401 (2010).
[45] M. U. Ubbens and P. A. Lee, Phys. Rev. B **46**, 8434 (1992).
[46] A. Rügg, M. Indergrand, S. Pilgram, and M. Sigrist, Eur. Phys. J. B **48**, 55 (2005).
[47] L. de'Medici, A. Georges, and S. Biermann, Phys. Rev. B **72**, 205124 (2005).
[48] P. Werner and A. J. Millis, Phys. Rev. Lett. **99**, 126405 (2007).
[49] S. Hoshino and P. Werner, Phys. Rev. B **93**, 155161 (2016).
[50] Y. M. Quan, L. J. Zou, D. Y. Liu, and H. Q. Lin, Eur. Phys. J. B **85**, 55 (2012).
[51] A. Sharoni, I. Asulin, G. Koren, and O. Millo, Phys. Rev. Lett. **92**, 017003 (2004).
[52] Q. Wang, Z. Li, W. Zhang, Z. Zhang, J. Zhang, W. Li, H. Ding, Y. Ou, P. Deng, K. Chang, J. Wen, C. Song, K. He, J. Jia, S. Ji, Y. Wang, L. Wang, X. Chen, X. Ma, and Q.Xue, Chin. Phys. Lett. **29**, 037402 (2012).
[53] D. Liu *et al.*, Nat. Commun. **3**, 931 (2012).
[54] S. He *et al.*, Nat. Mater. **12**, 605 (2013).
[55] W. Zhang *et al.*, Chin. Phys. Lett. **31**, 017401 (2014).
[56] J. J. Lee, F. T. Schmitt, R. G. Moore, S. Johnston, Y.-T. Cui, W. Li, M. Yi, Z. K. Liu, M. Hashimoto, Y. Zhang, D. H. Lu, T. P. Devereaux, D.-H. Lee, and Z.-X. Shen, Nature (London) **515**, 245 (2014).